J Neurophysiol 102: 2375–2386, 2009.
First published August 12, 2009; doi:10.1152/jn.00680.2009.

On the Origin of Event-Related Potentials Indexing Covert Attentional Selection During Visual Search

Jeremiah Y. Cohen, Richard P. Heitz, Jeffrey D. Schall, and Geoffrey F. Woodman
Department of Psychology, Vanderbilt Vision Research Center, Center for Integrative and Cognitive Neuroscience, Vanderbilt Brain Institute, Vanderbilt University, Nashville, Tennessee

Submitted 31 July 2009; accepted in final form 5 August 2009

Cohen JY, Heitz RP, Schall JD, Woodman GF. On the origin of event-related potentials indexing covert attentional selection during visual search. *J Neurophysiol* 102: 2375–2386, 2009. First published August 12, 2009; doi:10.1152/jn.00680.2009. Despite nearly a century of electrophysiological studies recording extracranially from humans and intracranially from monkeys, the neural generators of nearly all human event-related potentials (ERPs) have not been definitively localized. We recorded an attention-related ERP component, known as the N2pc, simultaneously with intracranial spikes and local field potentials (LFPs) in macaques to test the hypothesis that an attentional-control structure, the frontal eye field (FEF), contributed to the generation of the macaque homologue of the N2pc (m-N2pc). While macaques performed a difficult visual search task, the search target was selected earliest by spikes from single FEF neurons, later by FEF LFPs, and latest by the m-N2pc. This neurochronometric comparison provides an empirical bridge connecting macaque and human experiments and a step toward localizing the neural generator of this important attention-related ERP component.

INTRODUCTION

The electroencephalogram (EEG) has long been used as an electrophysiological measure of human brain activity (Berger 1929). Time-averaged event-related potentials (ERPs) derived from the EEG map onto diverse perceptual and cognitive states and processes (Rugg and Coles 1995). However, definitively identifying the neural generators of ERP components measuring specific cognitive operations has been intractable because the number of source configurations that can produce a given EEG voltage distribution on the scalp is infinite (Hillyard and Anllo-Vento 1998; Luck 2006; Nunez and Srinivasan 2006). Helmholtz (1853) proved that when the number of electrical generators is unknown, an infinite number of inverse solutions can account for any pattern of voltages across a sphere (like the head). Since the dawn of human electrophysiology, investigators have sought solutions to this inverse problem (Adrian and Matthews 1934; Walter 1938). Modern approaches infer the neural generators of human ERP components using source estimation algorithms (Nunez and Srinivasan 2006) or additional information from brain imaging (e.g., Heinze et al. 1994). However, this basic problem will remain underdetermined without constraints from intracranial recordings.

Intracranial recordings from epilepsy patients have provided useful information (Lachaux et al. 2003; Michel et al. 2004), but clinical and ethical constraints limit the general utility of this approach. Intracranial recordings can be carried out systematically and thoroughly in nonhuman primates. However, this is predicated on the homology of specific ERP components in humans and nonhuman primates. Several studies have identified ERP components in monkeys that are homologous to those in humans (Arthur and Starr 1984; Glover et al. 1991; Javitt et al. 1992; Lamme et al. 1992; Mehta et al. 2000a,b; Paller et al. 1992; Schroeder et al. 1991, 1992). Recently, we described a macaque homologue of the N2pc (an abbreviation of N2-posterior-contralateral, hereafter referred to as *m-N2pc*) (Woodman et al. 2007), an ERP component that measures the allocation of covert visual attention (Luck and Hillyard 1994a,b). We determined that the m-N2pc is maximal over extrastriate visual cortex and that the time and magnitude of the m-N2pc vary with visual search array set size. These properties parallel observations in humans.

The N2pc has been critical in distinguishing between models of attentional deployment during visual search because it provides a millisecond-by-millisecond measure of the focusing of attention in the left or right visual field (Woodman and Luck 1999, 2003b). The N2pc indexes a covert visual attention mechanism that is sensitive to the degree of distractor suppression required during visual search (Luck and Hillyard 1994a,b; Luck et al. 1997) and a perceptual selection mechanism that operates independent of later stages of processing (Woodman and Luck 2003a). When the N2pc was discovered, it was hypothesized to result from feedback from an attentional-control structure because this index of covert attention occurred after the earliest evidence for attentional selection found using spatial cuing paradigms (Heinze et al. 1994; Hopf et al. 2004; Luck and Hillyard 1994a). By establishing the homology between the N2pc in human and monkey, we can now test hypotheses about the origin of the N2pc.

To understand the dynamics of this component, we collected three measures of neural activity while macaque monkeys performed a difficult visual search task. We recorded intracranially from microelectrodes in the frontal eye field (FEF), an area in prefrontal cortex involved in covert visual selection hypothesized to represent a saliency map used to guide attention (Cohen et al. 2009a; Sato and Schall 2003; Sato et al. 2001; Schall 2004; Schall and Hanes 1993; Thompson and Bichot 2005; Thompson et al. 1997, 2005). The first neural measure was from the spike times of single neurons in FEF that discriminate between target and distractors during visual search. The second measure was from local field potentials (LFPs) recorded simultaneously with the single neurons that exhibit polarization differences for the target compared with distractors (Monosov et al. 2008). The LFP is believed to be a weighted average of dendrosomatic activity of about 10^5 neurons in approximately 1 mm^2 of cerebral cortex (Braitenberg

Address for reprint requests and other correspondence: J. D. Schall, Department of Psychology, Vanderbilt University, PMB 407817, 2301 Vanderbilt Pl., Nashville, TN 37240 (E-mail: jeffrey.d.schall@vanderbilt.edu).

and Schüz 1991; Katzner et al. 2009; Logothetis and Wandell 2004; Rockel et al. 1980). The third measure was the m-N2pc component, which is maximal over extrastriate visual cortex. ERP components have been estimated to arise from a weighted average of the LFPs summating from the synchronous activity of around 10^7 neurons in about 6 cm^2 of cortex (Cooper et al. 1965; Ebersole 1997; Nunez and Srinivasan 2006). These electrophysiological signals provide millisecond resolution of attention-related activity at multiple spatial scales.

By measuring these three signals we addressed a simple question: when the brain selects a target on which to allocate attention, does it happen all at once or through some sequence of processes at different scales in different places? The answer provides insight into the origin of the m-N2pc. If, under the conditions tested, the m-N2pc is driven by feedback from the selection process in FEF, then we should find that *1*) target selection in FEF precedes the m-N2pc and *2*) the amplitude of FEF activity correlates with the amplitude of the m-N2pc trial by trial.

METHODS

Behavioral task and recording

We recorded spikes from FEF neurons and LFPs from the same microelectrodes in both hemispheres of two male macaque monkeys (*Macaca radiata*, identified as Q and S). Simultaneously, we recorded ERPs from skull electrodes located at approximately OL/OR and T5/T6 in the human 10–20 system scaled to the macaque skull. In monkey S, we also recorded from anterior and middle electrodes corresponding to F3/F4 and C1/C2 in the human 10–20 system. The monkeys performed a memory-guided saccade task and a visual search task. In the search task, monkeys searched for a target (T or L in one of four orientations) among distractors (L or T). Distractors could be homogeneous (oriented uniformly) or heterogeneous (oriented randomly). Each trial began with the monkey fixating a central spot for about 600 ms. A target was then presented at one of eight isoeccentric locations equally spaced around the fixation spot (Fig. 1*A*). The other seven locations contained one, three, or seven distractor stimuli (set sizes 2, 4, and 8). The monkey was given a liquid reward for making a single saccade to the target location and fixating it for 1,000 ms. This single-saccadic-response criterion was used to ensure that the animals would process the search array prior to their response, enabling us to observe the deployment of covert attention to the target. Within sessions, trials with different set sizes were randomly interleaved. Across sessions the monkeys alternated between searching for Ts with Ls as distractors or Ls with Ts as distractors.

Activity from each neuron was recorded during a memory-guided saccade task to distinguish visual- from movement-related activity (Bruce and Goldberg 1985; Hikosaka and Wurtz 1983). The target was flashed alone for 80 ms. Monkeys were required to maintain fixation for 400–1,000 ms after the target onset. When the fixation spot disappeared, the monkey was rewarded for a saccade to the remembered location of the target.

Our data set consisted of 57 neurons from monkey Q and 23 neurons from monkey S, with simultaneously recorded LFPs and ERPs. Spikes were sorted on-line and off-line using principal-components analysis and template matching (Plexon). FEF LFPs were recorded from the same electrodes (2- to 5-MΩ impedance) as the single neurons, sampled at 1 kHz, and filtered at 0.7–170 Hz, using Plexon head-stage HST/8 050-G20 with an input impedance of 38 MΩ. EEG signals were sampled at 1 kHz and filtered between 0.7 and 170 Hz. A guide tube used with the microelectrodes, in contact with the surface of the dura, was used as reference for the LFP signal. The frontal EEG electrode (approximating human Fz) was used as reference for the EEG signal (Woodman et al. 2007).

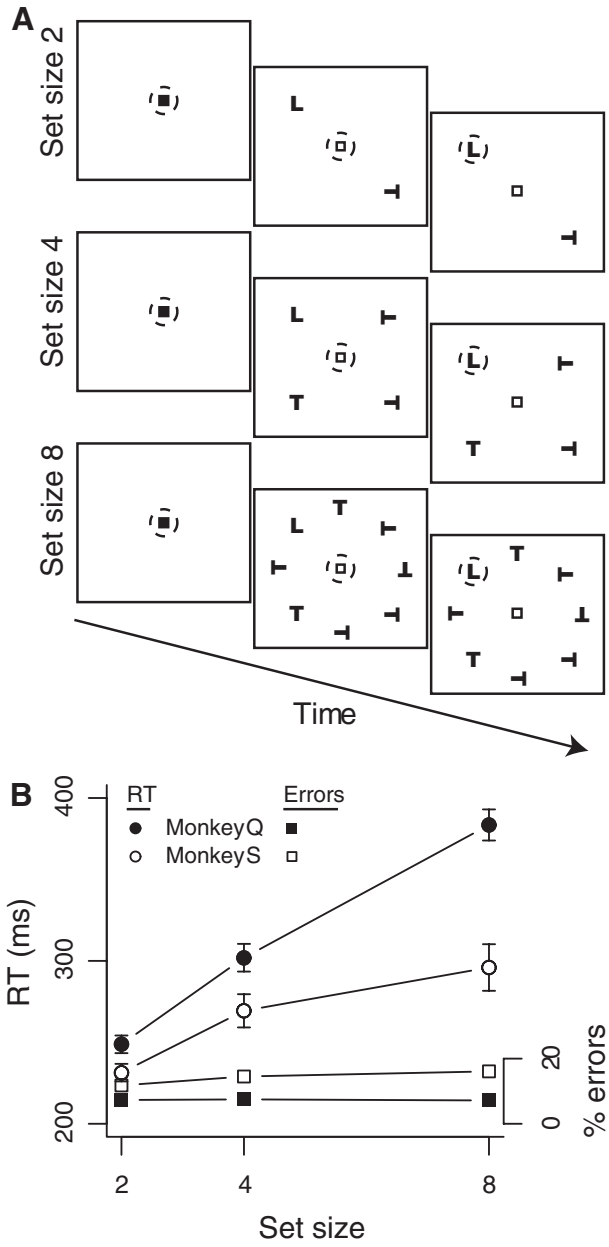

FIG. 1. Visual search task. *A*: monkeys made saccades to a target (here, an upright L; not to scale) presented with 1, 3, or 7 distractors. The monkey's eye position is represented by the dashed circle, which is invisible to the monkey. *B*: saccade response time (circles) and percentage error (squares) vs. set size for each monkey. Error bars represent SE around the mean of the session means. Filled symbols: monkey Q; open symbols: monkey S. Error bars for percentage error are smaller than plotted points.

Monkeys were surgically implanted with a head post, a subconjunctival scleral eye coil, EEG electrodes, and recording chambers under aseptic conditions with isoflurane anesthesia. Antibiotics and analgesics were administered postoperatively. All surgical and experimental procedures were in accordance with the Guide for the Care and Use of Laboratory Animals and approved by the Vanderbilt Institutional Animal Care and Use Committee.

Data analysis

To measure the firing rate of each neuron, we used a spike density function, convolving each spike with a kernel resembling a postsyn-

TABLE 1. *Comparisons of saccade response time, target selection time, and visual onset time*

	Monkey Q	Monkey S
Saccade response time, ms		
Set size 2	249.0 ± 5.4	231.0 ± 5.4
Set size 4	302.0 ± 8.5	269.0 ± 10.2
Set size 8	383.0 ± 9.5	296.0 ± 14.3
Slope of linear regression	22.1 ± 1.9**	10.2 ± 2.5**
Target selection time, ms		
Neuron	163.0 ± 4.2	156.0 ± 5.7
LFP	191.0 ± 3.9	169.0 ± 7.7
ERP	213.0 ± 4.6	191.0 ± 4.5
Neuron set size 2	177.0 ± 6.1	168.0 ± 8.4
Neuron set size 4	179.0 ± 5.7	189.0 ± 8.8
Neuron set size 8	194.0 ± 6.0	191.0 ± 9.2
LFP set size 2	203.0 ± 4.9	208.0 ± 14.3
LFP set size 4	221.0 ± 6.6	213.0 ± 15.7
LFP set size 8	234.0 ± 7.1	226.0 ± 16.1
ERP set size 2	206.0 ± 4.3	197.0 ± 7.1
ERP set size 4	235.0 ± 6.2	215.0 ± 8.2
ERP set size 8	266.0 ± 6.3	239.0 ± 8.6
Visual onset time, ms		
Neuron	72.0 ± 3.0	62.0 ± 4.0
LFP	54.0 ± 2.2	59.0 ± 4.3
ERP	67.0 ± 1.8	77.0 ± 1.8

Values are means ± SE. Pairwise comparisons are Wilcoxon signed-rank tests with significant differences highlighted: *$P < 0.05$; **$P < 0.001$.

aptic potential (Thompson et al. 1996). We used a memory-guided saccade task to classify neurons (Cohen et al. 2009b). Visual neurons had significantly greater activity in the 100 ms after the target flash than in the 100 ms before the target flash. Movement neurons had greater responses in the 100 ms leading up to the saccade than in the 100 ms before the target flash. Visuomovement neurons had greater responses in the 100 ms after the target flash and in the 100 ms leading up to the saccade than in the 100 ms before the target flash. Neurons analyzed in this study exhibited tonic visual and visuomovement activity with firing rates above baseline during the memory delay in the memory-guided task.

To measure the time of target selection, we used millisecond-by-millisecond Wilcoxon rank-sum tests. Selection time is defined as the time at which the distribution of activity when the search target was inside a neuron's receptive field (RF) was significantly greater than the distribution of activity when the target was opposite the receptive field for 10 consecutive milliseconds with $P < 0.01$. This "neuron–antineuron" approach (Britten et al. 1992; Thompson et al. 1996) presumes that a population of neurons in the brain representing the location of the target competes with a population of neurons representing the location of distractors opposite the target. No difference in target selection time was seen between visual neurons and visuomovement neurons.

We measured target selection time in LFPs and ERPs similarly. The beginning of the m-N2pc is simply the target selection time in ERPs as defined earlier. Because ERPs do not have receptive fields per se, we did two kinds of comparisons. The first comparison was based on the RF of the neuron recorded simultaneously with the ERP; we measured the difference between the ERPs on trials when the search array target was inside the single neuron's RF and the ERPs on trials when the target fell at the location(s) opposite the neuron's RF. The second comparison was the more typical approach used in ERP research: we measured the difference between the ERPs on trials when the target was in the hemifield contralateral to the EEG electrode and the ERPs on trials when the target was in the hemifield ipsilateral to the EEG electrode. Of the 80 recording sessions, each neuron selected the target of search, 56 LFPs selected the target, and 77 ERPs selected the target. Thus for the paired comparisons of simultaneously recorded neurons and LFPs (and LFPs and ERPs) the sample size was 56.

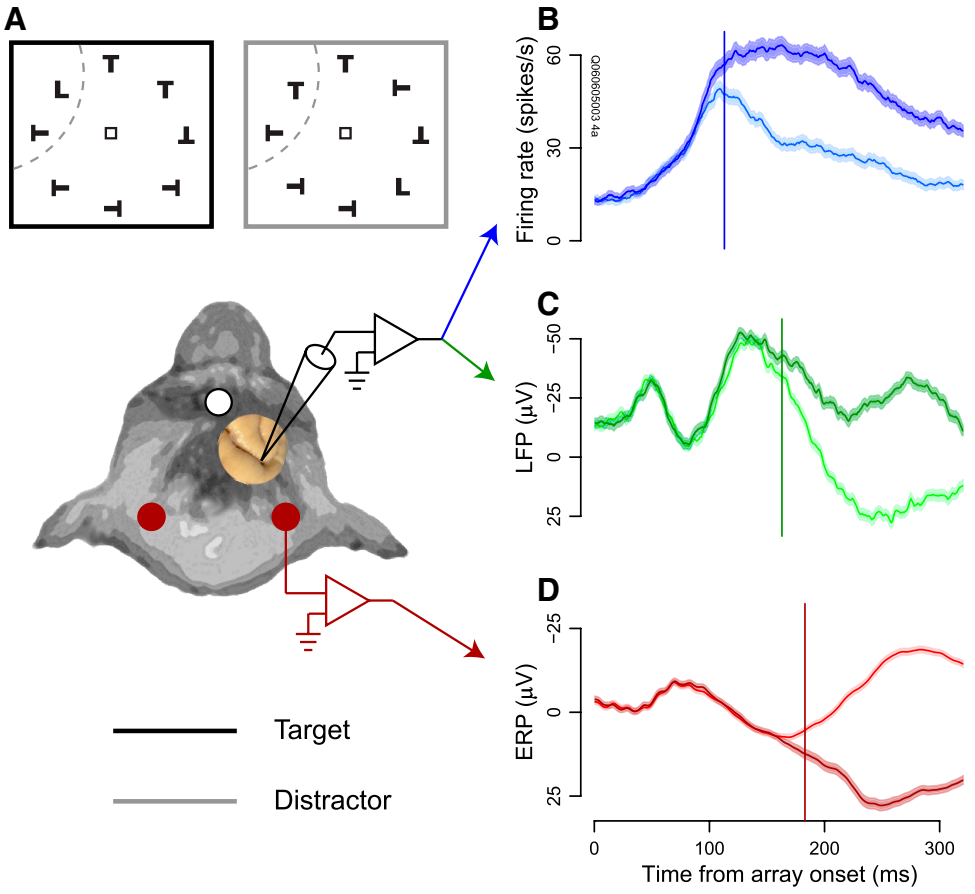

FIG. 2. Target selection during a representative session. *A*, *top*: visual search display (shown here with a set size of 8) with the target (L) inside the neuron's receptive field (indicated by the dashed arc) (*left*) and opposite the receptive field (*right*). *Bottom*: schematic of recording sites and signals. Single-unit discharges (blue) and local field potentials (green) were recorded intracranially from frontal eye field (FEF). Event-related potentials (ERPs) were recorded from electrodes over extrastriate visual cortex (red). *B*: average activity of one neuron when the search target was inside (dark) and opposite (light) its receptive field. Bands around average firing rates show time-varying SE. Vertical line indicates *target selection time* when the 2 curves became statistically significantly different. *C*: FEF local field potential (LFP) with the target inside (dark) and opposite (light) the simultaneously recorded neuron's receptive field (RF). *D*: ERP over extrastriate visual cortex from trials with the target inside (dark) and opposite (light) the receptive field of the concomitantly recorded FEF neuron. This component is the macaque homologue of the human N2pc (m-N2pc).

We also measured the trial-by-trial correlation in the amplitude of modulation of spike rate, LFP polarization, and ERP polarization in the 56 spike–LFP–ERP triplets in which all three signals selected the target. We computed a Pearson correlation coefficient for each simultaneously recorded spikes–ERP (and spikes–LFP) pair using the trial-by-trial spike rate and integral of ERP (or LFP) amplitude in a window from 150 ms after the search array appeared until saccade initiation (to exclude the initial nonselective visual response), divided by the length of the time window. Similarly, we computed the correlation for each LFP–ERP pair using the trial-by-trial integral of the amplitude in the same time window, divided by the length of the window.

To measure the onset time of visual activity in each signal, we compared baseline activity in the 100 ms before search array onset to each millisecond of activity after array onset. We used millisecond-by-millisecond Wilcoxon rank-sum tests to compare the two distributions. To ensure that our measurements of covert attentional selection were not an artifact of the overt response required to perform the task we also analyzed the signals truncated 20 ms prior to the saccade response. These analyses yielded the same pattern of results. Visual onset time was defined as the first time when activity after array onset exceeded baseline activity for 10 consecutive milliseconds with $P < 0.01$. All statistical tests were done with Bonferroni corrections for multiple comparisons. All analyses were done with R (http://www.r-project.org/; Cohen and Cohen 2008).

RESULTS

Behavior

Two monkeys searched for a target stimulus among one, three, or seven distractor stimuli (set sizes 2, 4, and 8) composed of the same basic features in a T/L search display (Fig. 1*A*). Both monkeys responded to larger set sizes with longer saccade response times (Fig. 1*B*, Table 1), demonstrating the attentional demands of the task (Cohen et al. 2009a; Duncan and Humphreys 1989; Treisman and Gelade 1980).

Target selection time

We recorded spiking activity from 57 neurons in monkey Q and 23 neurons in monkey S, simultaneously with LFPs in FEF

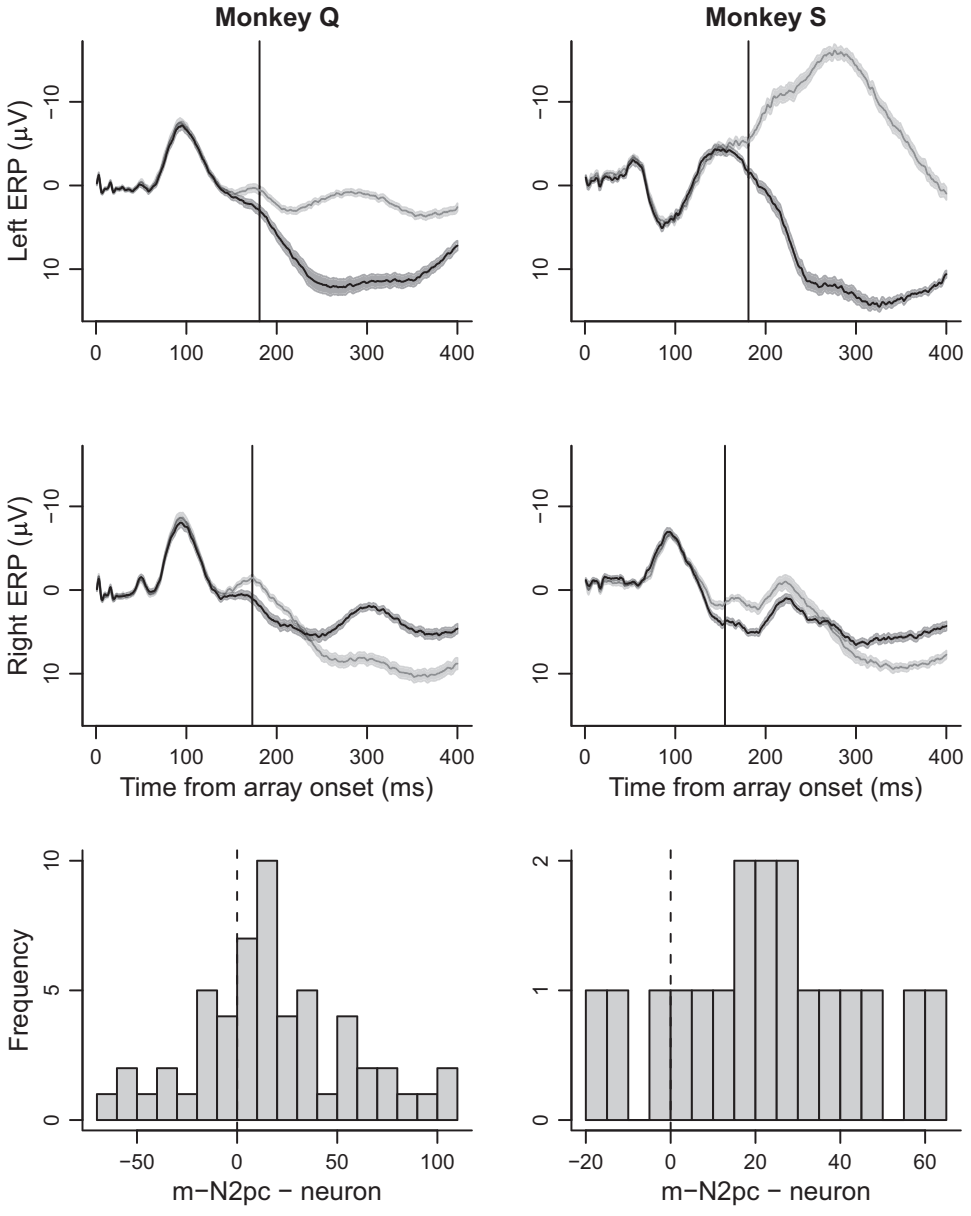

FIG. 3. Average left (*1st row*) and right (*2nd row*) hemisphere ERPs with the search target in the hemifield contralateral (dark curves) and ipsilateral (light curves) to the recording site. Bands around activity curves indicate SE. Solid vertical lines indicate onset of the m-N2pc. The *bottom row* shows histograms of m-N2pc minus single-neuron selection times for each monkey, in which m-N2pc was computed using contralateral vs. ipsilateral target responses. Despite the increased number of trials associated with the m-N2pc, single-neuron spikes selected targets earlier than the hemisphere-based m-N2pc (Wilcoxon signed-rank test, $P < 0.001$ for each monkey). Dashed vertical lines indicate zero difference between m-N2pc and neuron.

and the m-N2pc from EEG electrodes over extrastriate visual cortex. Each neuron exhibited visual responses and sustained activity during a memory-guided saccade task. We compared *target selection time* in each of the three measures of neural activity, defined as the time at which each signal discriminated between the target and distractors.

Figure 2 shows representative simultaneous recordings of spikes and LFPs in FEF and the m-N2pc in the ERP over extrastriate visual cortex. The FEF neuron initially responded at the same rate when the target or only distractors appeared in its RF but then evolved to select the target of search by increasing discharge rate when the target was in its RF relative to when a distractor was in its RF. The concurrently recorded LFP exhibited an equivalent early polarization when the target was in the neuron's RF relative to when only distractors were in the neuron's RF followed by a greater negativity for the target relative to distractors. Likewise, the simultaneously recorded visual ERP over extrastriate visual cortex exhibited an initial period of unselective polarization in response to the search array, but eventually showed a more positive polarization when the target appeared inside the simultaneously recorded neuron's RF relative to when a distractor appeared in the neuron's RF (the m-N2pc). Thus qualitatively, each level and location of electrophysiological signal underwent the same state change from nonselective to a selective representation. However, this state change occurred at different times for each level of electrophysiological signal. A differential signal sufficient to locate the target occurred earliest in the spikes of the FEF neuron (113 ms after search array onset), later in the FEF LFP (163 ms), and latest in the visual ERP (183 ms). This was also observed in comparisons of all trials with the target contralateral compared with those with the target ipsilateral to the EEG electrode (Fig. 3).

Figure 4*A* demonstrates that this sequence of target selection was a common observation across the sample of sessions with different neurons recorded with LFPs at different sites in FEF and with the same posterior EEG electrodes. Overall, the target was selected significantly earlier by FEF single-neuron spikes (mean ± SE, 161 ± 3.4 ms) than by FEF LFPs (184 ± 3.7 ms) (Wilcoxon signed-rank test, $P < 0.001$), as observed previously (Monosov et al. 2008). Moreover, single neurons in FEF selected the target before the m-N2pc (207 ± 3.7 ms) ($P < 0.001$). Likewise, the target was selected significantly earlier by FEF LFPs than by the ERPs, as reflected by the m-N2pc ($P < 0.001$; Table 1). This sequence of target selection timing was highly reliable within recording sessions for both monkeys (Figs. 4 and 5; Table 1). The average difference between FEF single-neuron selection time and LFP selection time was 31 ± 5.4 ms for monkey Q and 13 ± 5.9 ms for monkey S. The average difference between LFP selection time and the m-N2pc was 18 ± 4.3 ms for monkey Q and 22 ± 8.6 ms for monkey S, and the average difference between neuron selection time and the m-N2pc was 49 ± 5.6 ms for monkey Q and 37 ± 6.3 ms for monkey S.

To ensure that the delay of LFP and ERP signals relative to the spike rate modulation was not an artifact of the recording procedures, we measured the latency of the earliest visual response in each neural signal. The earliest visual response was observed in FEF LFPs (Table 1), in agreement with a recent study of the relationship between visually responsive neurons and concurrently recorded LFPs (Monosov et al. 2008). The

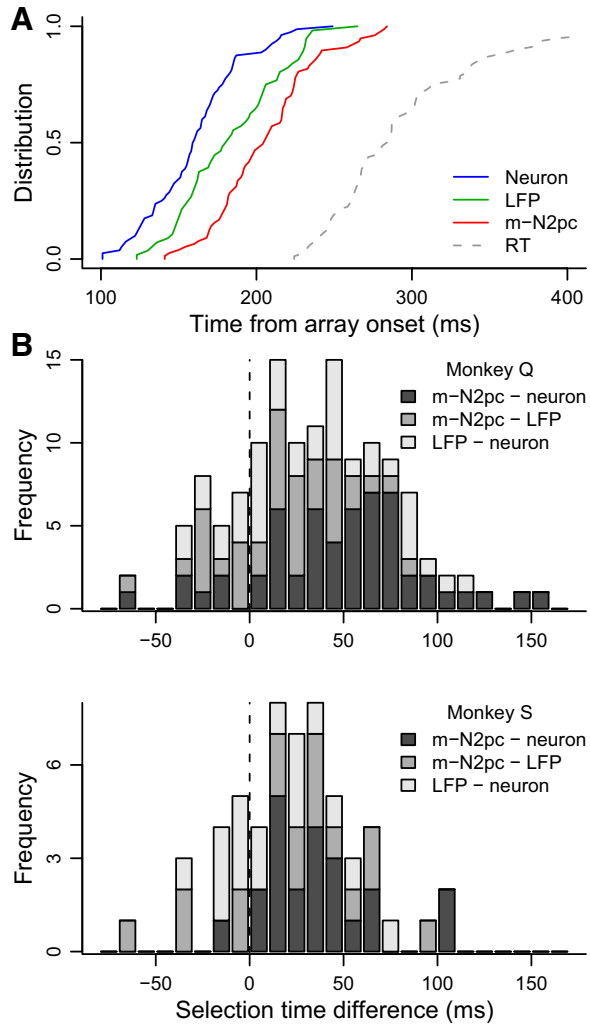

FIG. 4. Target selection time differences. *A*: cumulative distributions of target selection times measured from simultaneously recorded intracranial FEF neuron spike times (blue) and FEF LFPs (green) with extracranial m-N2pc (red). These events precede the saccade response times (RTs, dashed gray curve). *B*: stacked histograms showing differences between target selection time measured from simultaneously recorded m-N2pc and single-neuron spikes (dark gray), m-N2pc and LFPs (gray), and LFPs and single-neuron spikes (light gray) for each monkey. Most of the values exceed zero, indicated by the dashed vertical line.

latencies of the initial nonselective visual ERP component were similar to those observed in extrastriate areas such as V4 (Schmolesky et al. 1998). Across monkeys, the onset of the earliest visual response was 57 ms for the FEF LFPs, 67 ms for FEF neurons, and 72 ms for the posterior visual ERPs. Thus the differences we observed in the timing of attentional selection signals cannot be explained by inherent differences in when the first visual activity was observed across the different signals.

Results of these analyses are consistent with the hypothesis that feedback from FEF contributes to the generation of the m-N2pc component. This was tested further by assessing whether the target selection time in FEF and the m-N2pc varied in parallel with search array set size and saccade response time.

Set-size effects

As noted earlier, both monkeys produced longer saccade response times with larger set sizes (Fig. 1*B*, Table 1). The

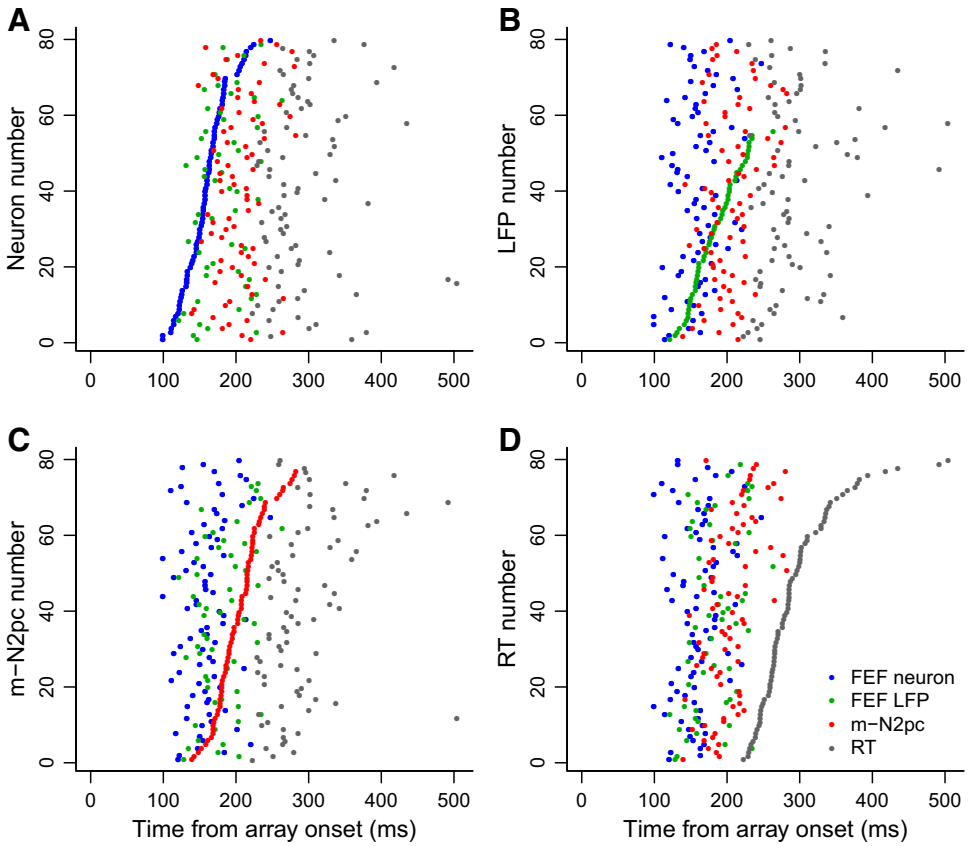

FIG. 5. Target selection time within sessions sorted by neuron selection time (*A*), LFP selection time (*B*), m-N2pc (*C*), and saccade RT (*D*). Each row corresponds to one recording session, with FEF single-neuron selection time in blue, FEF LFP selection time in green, visual cortex ERP selection time (m-N2pc) in red, and mean saccade RT in that session in gray.

single-unit recordings show that a delay in the time for FEF neurons to locate the target predicted the increase of saccade response time with set size (Cohen et al. 2009a) (Fig. 6). Next, we determined the extent to which delays of target selection by LFPs and the m-N2pc predicted the delay of saccade response time. Figure 6 shows that the time of target selection was delayed with increasing set size measured through single FEF neurons (linear regression slope 3.0 ± 1.4 SE ms/item for monkey Q, 2.7 ± 2.3 ms/item for monkey S), FEF LFPs (5.0 ± 1.9 Q, 3.0 ± 4.0 S), and the m-N2pc (9.6 ± 1.4 Q, 6.8 ± 1.8 S). Thus increasing the set size led to delayed target selection for the FEF activity and the m-N2pc. Note that this delay was significantly greater for the m-N2pc than that for FEF LFPs or single neurons.

Trial-by-trial correlation of spike rate, LFP, and ERP amplitude

If FEF contributes to the generation of the m-N2pc measured over extrastriate visual cortex, then the amplitude of FEF activity and posterior ERPs should covary across trials. We used FEF single-neuron spikes, FEF LFPs, and the extrastriate ERPs that selected the target from distractors and computed the correlation coefficients from trials in which the target was inside the neuronal RFs. The trial-by-trial correlation between the spike rate of individual neurons in FEF and the integral of ERP amplitude was significant in just 4 of the 56 pairs (Fisher's z test, $P < 0.05$; Fig. 7*A*). In contrast, the trial-by-trial correlation between the integral of FEF LFP and extrastriate ERP amplitude was significant in 34 of the 56 pairs (Fisher's z test, $P < 0.05$; Fig. 7*B*). In addition, the LFP–ERP correlation coefficients were significantly larger when the target fell within the RFs (mean $r \pm$ SE, 0.26 ± 0.02), compared with when only distractors fell within the RFs (0.19 ± 0.02) (Wilcoxon signed-rank test, $P < 0.05$). The lack of correlation between spikes and ERPs was not a result of comparing different signal types. The trial-by-trial correlation between spikes and LFPs was significant in 32 of the 56 pairs (Fisher's z test, $P < 0.05$; Fig. 7*C*). These amplitude correlations between FEF LFPs and posterior ERPs support the hypothesis that FEF contributes to the generation of the m-N2pc.

Signal and noise in each measure of neural activity

Although the timing of target selection by FEF neurons and LFP relative to the extrastriate ERPs is consistent with the hypothesis that the m-N2pc is driven by feedback from the selection process in FEF, we wanted to rule out a simple alternative explanation. The pattern of target selection times could just be a difference inherent in the neural measures at different spatial scales. In particular, the signal-to-noise characteristics of the spike times of single neurons may be different from the signal-to-noise characteristics of an LFP (derived from $\sim 10^5$ neurons) and from the signal-to-noise characteristics of an ERP component (derived from $\sim 10^7$ neurons). It may be that through summation the LFP and ERP become more reliable measures. Alternatively, the summation may introduce more noise into the LFP and ERP. To quantify the reliability of the signals at each spatial scale, we computed target selection time for each signal as a function of number of trials (Fig. 8, *A* and *B*). The estimate of target selection time tends to decrease with the number of trials contributing to the

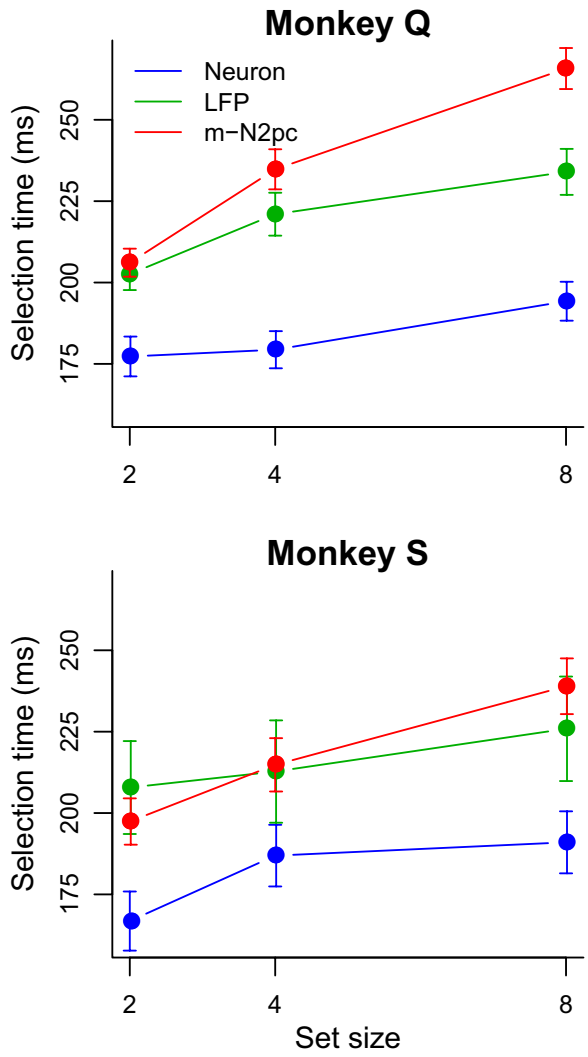

FIG. 6. Target selection time mean and SE for FEF single-neuron spikes (blue), FEF LFPs (green) and m-N2pc (red) for each set size for each monkey.

calculation until an asymptote is reached (Bichot et al. 2001). We reasoned that target selection time would vary with trial number according to the signal-to-noise characteristics of the signals at different spatial scales. We fit an exponential function to the average curves of FEF single-neuron selection time, FEF LFP selection time, and the m-N2pc, $TST = TST_{max+min} e^{-n/\tau} + TST_{min}$, where TST is target selection time; n is the number of trials; and τ, $TST_{max+min}$, and TST_{min} are the decay (in units of trials), baseline (ms), and asymptote (ms) parameters that were free to vary. The mean decay parameter $\tau \pm$ SE was 336 ± 96 trials for neurons, 308 ± 75 trials for LFPs, and 432 ± 125 trials for the m-N2pc for monkey Q, and 423 ± 224 trials for neurons, 209 ± 39 trials for LFPs, and 358 ± 245 trials for the m-N2pc for monkey S (Fig. 8*C*). These values were not significantly different from one another (Wilcoxon rank-sum test, $P > 0.1$). The mean $TST_{min} \pm$ SE was 139 ± 12 ms for neurons, 156 ± 6 ms for LFPs, and 157 ± 14 ms for the m-N2pc for monkey Q, and 134 ± 12 ms for neurons, 131 ± 80 ms for LFPs, and 164 ± 26 ms for the m-N2pc for monkey S (Fig. 8*D*). For monkey Q, TST_{min} was significantly smaller for neurons than for LFPs and ERPs (Wilcoxon rank-sum test, $P < 0.01$). For monkey S, TST_{min} was significantly smaller for neurons than for ERPs and for LFPs than for ERPs (Wilcoxon rank-sum test, $P < 0.01$), corresponding to the differences in target selection time reported earlier (Fig. 4; Table 1).

These fits show that the asymptote of target selection time was reached with fewer trials than the number of trials sampled in our data set (indicated by the black point and horizontal error bars in Fig. 8*B*). We next compared selection times across the three measures for varying numbers of sampled trials. When the number of trials exceeded 400, FEF single-neuron selection

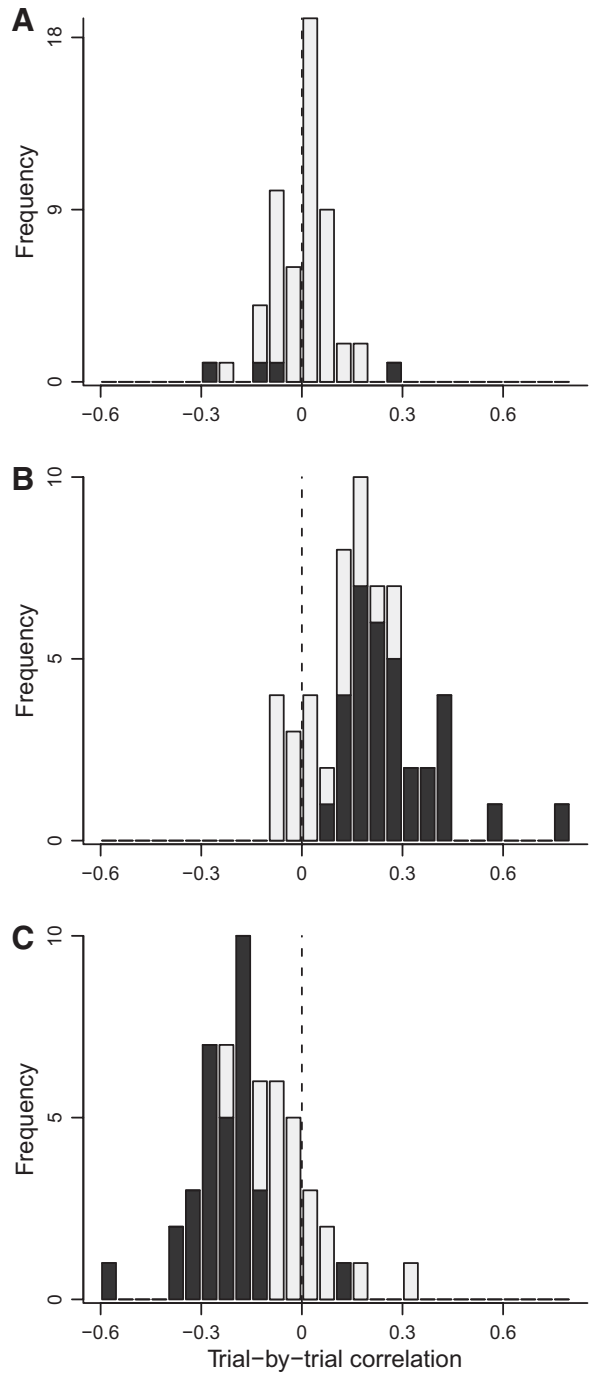

FIG. 7. Trial-by-trial correlation between spike rates and ERP amplitude (*A*), between LFP and ERP amplitude (*B*), and between spike rates and LFP amplitude (*C*). Significant correlation coefficients are shown in dark bars (Fisher's z test, $P < 0.05$). Dashed vertical lines indicate a correlation of zero.

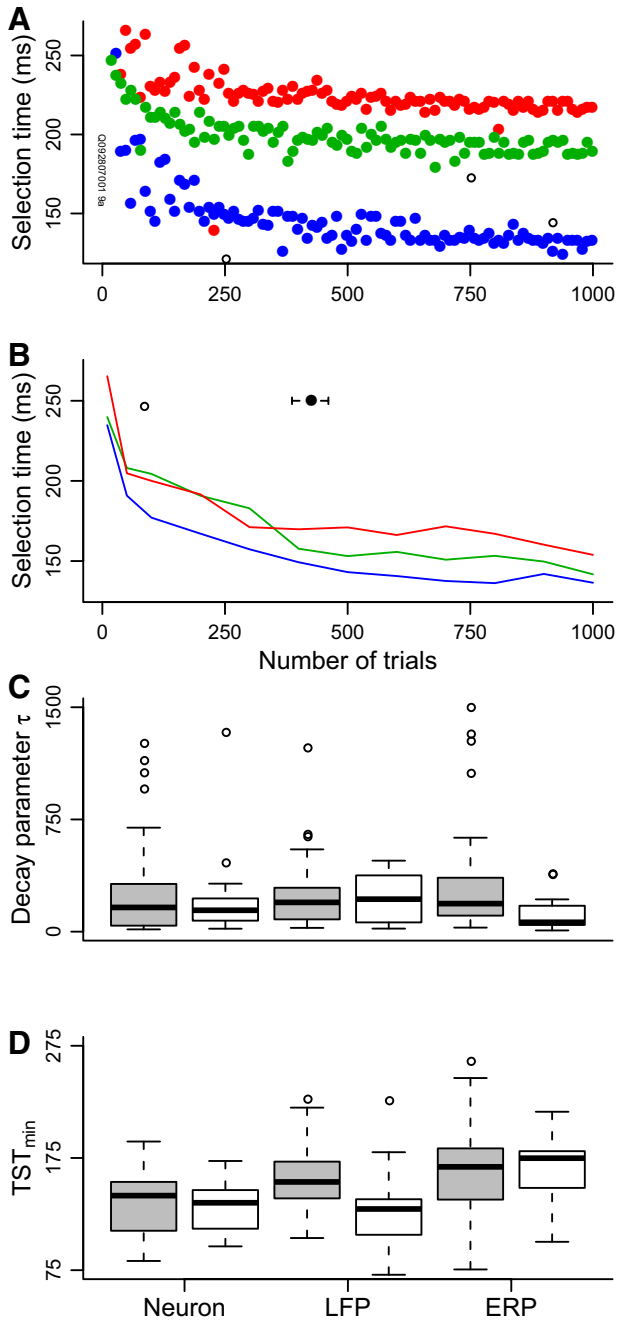

FIG. 8. Target selection time as a function of number of trials. *A*: target selection time estimates as a function of randomly sampled (without replacement) trials from an example recording of an FEF single neuron (blue), FEF LFP (green), and extrastriate visual cortex ERP (m-N2pc; red). *B*: average target selection time estimates as a function of randomly sampled (with replacement) trials across recordings for FEF neurons (blue), FEF LFPs (green) and m-N2pc (red). The black point with SE bars indicates the number of trials sampled in our data set. *C*: decay parameter estimates from exponential fits to the selection time × number of trials curve for each session. Gray boxes are from monkey Q, white boxes from monkey S. *D*: asymptote parameter estimates from the same exponential fits as in *C*.

time was significantly earlier than FEF LFP selection time and FEF LFP selection time was significantly earlier than the m-N2pc (Wilcoxon signed-rank tests, $P < 0.05$). These findings are consistent with the observation that the SEs of the means for the signals at each spatial scale were comparable (Fig. 2). Therefore the timing differences across the electrophysiological indices of attentional selection seem not to be an artifact of different signal-to-noise characteristics of the signals at different spatial scales.

Spatial distribution of the m-N2pc

To evaluate the possibility that dipoles in FEF contributed to the posterior ERPs, we measured ERPs from anterior, middle, and posterior pairs of lateralized electrode sites. As shown previously, the m-N2pc is not observed on anterior electrodes (Woodman et al. 2007). This is so despite the clear evidence of a target-selection process in LFPs recorded in FEF beneath these anterior surface electrode pairs (Fig. 9). Apparently, the LFPs in FEF do not create a dipole with the proper geometry to be observed on EEG electrodes over frontal cortex. This is not surprising, given the anatomical location of FEF in the rostral bank of the arcuate sulcus with pyramidal neurons oriented close to parallel to the surface of the skull.

If the LFPs generated in FEF create an electrical dipole oriented perpendicular to the pial surface of the frontal lobe, then this would result in a rostrocaudally oriented electrical field. Such an electric field could produce surface voltage density gradients over the parietal or occipital lobe. Thus it is possible that the m-N2pc is really a manifestation of the volume conduction of the FEF dipole. However, if this were the case, then because electrical signal conduction is essentially instantaneous in the conductive medium of the brain (Nunez and Srinivasan 2006), the m-N2pc should occur instantaneously with the FEF LFPs. This was not the case under the conditions of this experiment.

Shape of the ERP

ERPs over posterior cortex show a transient negative polarization in response to a visual stimulus in humans and monkeys known as the N1 component (Woodman et al. 2007). Curiously, a craniotomy over FEF in monkey S inverted the N1 to a positive polarization in the left hemisphere but not the right (Fig. 3). Note that the m-N2pc was not inverted; it remained a positive polarization. Importantly, the m-N2pc timing was not significantly different between left and right hemispheres for either monkey (Wilcoxon rank-sum test, $P > 0.2$ for each monkey), although the shape of the target-selection signal was different between left and right hemispheres for each monkey (Fig. 3).

Signal distortion by the recording circuit

Recent work has shown that LFPs are distorted by the intrinsic filtering characteristics of high-impedance microelectrode recording circuits (Nelson et al. 2008). This distortion is systematic and can be corrected. An example corrected LFP is shown in Fig. 10. Target selection time was not significantly different between corrected and uncorrected LFPs. Because of this lack of difference in selection times, we report values drawn from the raw, uncorrected LFPs, to compare directly to a previous study (Monosov et al. 2008). The impedance of the EEG electrodes, 2–5 kΩ measured at 30 kHz, was sufficiently low that it caused minimal signal distortion; indeed, when we applied the correction to ERPs, we saw no difference in target selection time between uncorrected and corrected signals.

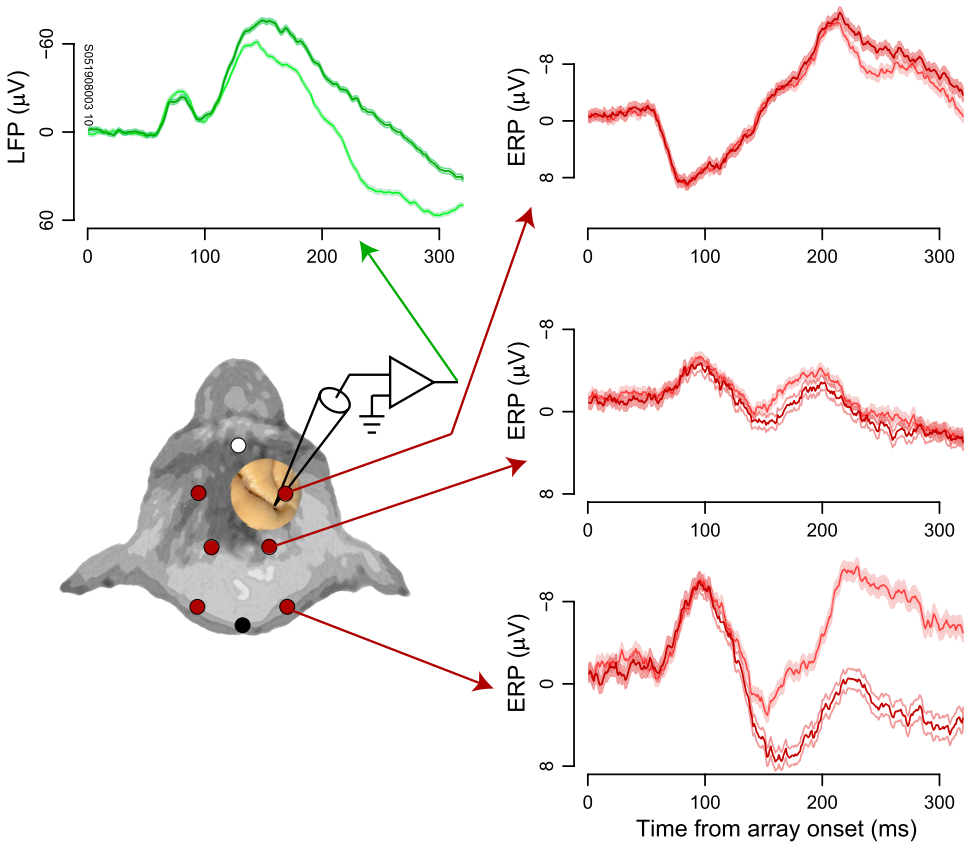

FIG. 9. Spatial distribution of ERPs shown with FEF LFP from an example recording session in monkey S. Dark curves represent potentials when the target was contralateral to the recording site (i.e., left visual field), light curves represent potentials when the target was ipsilateral to the recording site (i.e., right visual field). Bands around activity curves indicate SE. The anterior electroencephalographic (EEG) electrode was embedded in the skull, but is displayed here on top of the exposed cortical surface for purposes of illustration.

DISCUSSION

To create a bridge between research investigating attentional selection using human ERPs and research using macaque intracranial electrophysiology, we recorded the putative macaque homologue of the N2pc component indexing covert selection simultaneously with spikes from single neurons and LFPs in FEF. We show that visual targets are selected by FEF spikes and LFPs earlier than the ERP component that is maximal over extrastriate visual cortex. Thus our findings support the hypothesis that the N2pc is generated due to feedback from an attentional-control structure (such as FEF) because in this visual search task the target is located by FEF before it is located by the m-N2pc. Before accepting this conclusion, we discuss three alternative explanations that can be ruled out.

First, the signal-to-noise characteristics of the spike times of single neurons may be different from the signal-to-noise characteristics of the ensemble activity measured with LFPs and ERPs. However, as shown earlier (Fig. 8), the three electrophysiological measures of target selection time exhibited similar reliability as a function of the number of trials sampled. If one of the signals were more reliable across trials, then the estimate of target selection time would have reached asymptote with fewer trials sampled. Not observing any difference is consistent with the basic observation of similar variability in the different signals (Fig. 2, Table 1) and rules out the possibility that the differences in timing were simply due to greater intrinsic signal-to-noise differences in the ERPs or LFPs relative to the neurons. This finding has implications for neural prosthetics. If the signal-to-noise ratio of spikes, LFPs, and ERPs are similar, then the ability to decode an appropriately chosen ERP will be similar to that of spikes.

Second, the difference in voltage polarity between human N2pc (negative) and macaque m-N2pc (positive) could mean that these potentials are measuring different underlying ERP components. However, this proposition would need to explain why the m-N2pc and the human N2pc have such similar timing (Figs. 2–5), task dependence (Fig. 6), and spatial distribution (Fig. 9). On the other hand, the difference in polarity can be explained by the difference in anatomy. The neural generator of the human N2pc is thought to include area V4 (Hopf et al. 2000; Luck et al. 1997). Macaque V4 is located partially on the surface of the prelunate gyrus (Gattass et al. 1988; Zeki 1971), whereas the human homologue of V4 is buried in a region containing multiple sulci and gyri (Orban et al. 2004; Sereno et al. 1995; Tootell and Hadjikhani 2001). Thus it is plausible that the m-N2pc has the opposite polarity of the human N2pc because of the differences in cortical folding between species. Indeed, similar reasoning about the contribution of cortical folding to the polarity of ERPs applies to at least two other ERP components. The human C1 has a negative polarity when a visual stimulus is presented above the horizontal meridian and a positive polarity when a stimulus is presented below the horizontal meridian, consistent with the shape of the calcarine sulcus (Clark et al. 1995). The lateralized readiness potential has a negative polarity preceding hand movements and a positive polarity preceding foot movements, consistent with the opposing locations of the hand (lateral) and foot (medial) representations in primary motor cortex (Brunia and Vingerhoets 1980; Leuthold and Jentzsch 2002). Thus based on differences in cortical folding between macaques and humans,

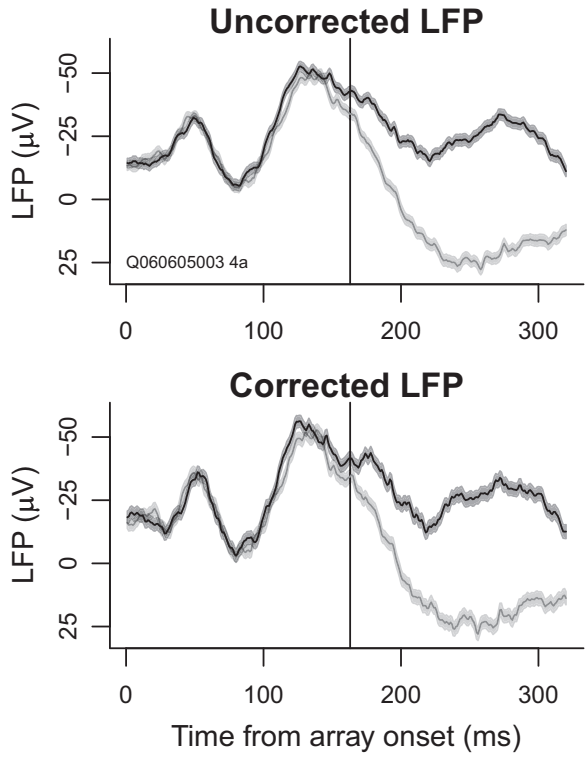

FIG. 10. Signal distortion by the recording circuit. The *top panel* shows the raw LFP with the target inside (dark) and opposite (light) the simultaneously recorded neuron's RF; this is from the example session in Fig. 2. The *bottom panel* shows the corrected LFP using an empirical estimate of the recording circuit's transfer function obtained from a procedure described in Nelson et al. (2008). Target selection time was not significantly different between corrected and uncorrected LFPs. Vertical lines indicate target selection time measured using the uncorrected LFPs. Bands around activity curves indicate SE.

we believe that the m-N2pc is homologous to the human N2pc. We also considered the possibility that the m-N2pc could be generated from a rostrocaudally oriented dipole in the macaque FEF. However, the timing differences between target selection in the FEF LFP and the m-N2pc are inconsistent with this hypothesis. It is likely that the FEF dipole is actively cancelled out by electrical fields with similar timing and of opposite polarity generated in neighboring cortical areas or in brain areas that lie between FEF and the posterior electrodes above extrastriate visual cortex (e.g., the lateral intraparietal area). This latter source of active cancellation of the FEF dipole would be consistent with a magnetoencephalography study of the N2pc component in humans, showing that the N2pc over ventral visual cortex is preceded by an activation in posterior parietal cortex (Hopf et al. 2000).

Third, one might hypothesize that an ERP component recorded outside the brain arises with some delay after the synaptic events in the dipole source producing that ERP component. We can reject this hypothesis because, whereas EEG is subject to spatial distortion, it is not delayed relative to synaptic activity (Nunez and Srinivasan 2006). Thus the remaining and most plausible hypothesis is that, under the conditions tested, target selection in FEF precedes that of the m-N2pc.

Our results demonstrate that the brain selects a target during visual search through a sequence of processes manifesting in the frontal lobe before posterior visual areas. This attentional cascade occurs in the spike rates of single neurons in FEF before the selective polarization of intracranial LFPs and the ERPs recorded through the skull, which represent a summation of field potentials in the brain. This shows that the N2pc component in primates does not index the earliest time that the brain selects a visual search target to receive the benefit of attention. This is consistent with evidence suggesting that areas that perform spatial visual selection lead those that perform detailed processing of object identity (Hopf et al. 2000).

These findings bear on hypotheses about the functional architecture of attention and visual search. The larger increase in m-N2pc onset than target selection time in FEF as a function of set size (Fig. 6) is consistent with the hypothesis that the selection process in a putative saliency map (such as FEF) takes less time than the focusing of visual attention performed in the areas generating the m-N2pc (Luck and Hillyard 1994b). Attentional models of visual search such as Guided Search (Wolfe 2007) propose that increased activity in the saliency map precedes the effects of focusing visual attention on the target representation in extrastriate visual cortex, resulting in the binding of target features.

We also rule out a simple feedforward architecture, in which visual signals propagate only from visual cortex to frontal cortex. The data support theories of attention that propose that top-down input from frontal cortex guides attentional selection in visual cortical areas (Bundesen et al. 2005; Desimone and Duncan 1995; Lamme and Roelfsema 2000). FEF is situated chronometrically and anatomically to influence areas such as V4 and IT (Barone et al. 2000; Gregoriou et al. 2009; Schmolesky et al. 1998) and it appears that target-selecting neurons in FEF may be a major source of signals to extrastriate visual cortex (Pouget et al. 2009). The potency of this signal has been demonstrated in humans and macaques. Transcranial magnetic stimulation over human FEF biases attention in the corresponding part of space and visual ERPs (Juan et al. 2008; Taylor et al. 2007) and microstimulation of macaque FEF biases attention and activity in extrastriate visual cortex (Armstrong et al. 2006). Finally, our results provide the first direct test of the hypothesis that the N2pc is due to feedback from an area that controls the focus of visuospatial attention (Luck and Hillyard 1994b). The timing of this feedback may depend strongly on task demands. A recent study reported that attentional modulation occurred on average 8 ms earlier in FEF neurons than in V4 neurons (Gregoriou et al. 2009), although this measurement had a large amount of variability. Our results indicate nearly an order-of-magnitude greater time difference (ranging from ~30 to 70 ms depending on set size). This difference may have arisen from a difference in the attentional demands of the task or the contribution of other areas in extrastriate or parietal cortex to the m-N2pc. Gregoriou et al. (2009) suggested that the 8-ms delay corresponded to the axonal transmission time between FEF and V4. However, the reliability of axonal conduction cannot explain the degree of variability in their estimate. The time differences we measured are long enough to permit axonal conduction plus synaptic integration, which seems more plausible for an interaction of the sort described by models of top-down processing.

In addition to our conclusions about the relationship between FEF and the m-N2pc, we also replicated a recent finding in FEF: LFPs select visual targets later than the simultaneously recorded spikes (Monosov et al. 2008). This may seem counterintuitive; if the LFP represents synaptic potentials that lead

to spikes, then one might expect them to show target selection before spikes. Indeed, the initial visual responses were earlier in the LFPs than in the spikes (Table 1). However, the later target selection times in LFPs than those in spikes suggests that FEF LFPs reflect nonselective visual inputs to FEF neurons, whereas FEF spikes reflect the outcome of target selection that is computed in FEF itself.

Despite this seemingly clear dissociation between FEF inputs and outputs, our results also challenge the view that LFPs represent only the synaptic input to a region of cortex. We observed a strong trial-by-trial correlation between FEF LFPs and posterior ERPs, but not between FEF spikes and posterior ERPs (Fig. 7). If spikes represent output from a cortical area and LFPs represent strictly input, then these correlations could reflect that the neural generator of the m-N2pc also projected to FEF but that FEF did not project directly to the neural generator of the m-N2pc. Because the projection from FEF to extrastriate cortex is strong (Barone et al. 2000; Pouget et al. 2009) and it is likely that many of the neurons we recorded projected to extrastriate cortex (see Fig. 5 in Thompson et al. 1996), this explanation seems unlikely. Thus we propose that the weak correlations between spikes and ERPs reflect the weak relationships between these signals. Indeed, several studies have shown weak relationships between spikes and slow-wave EEG (Buchwald et al. 1965; Fromm and Bond 1964, 1967; Marsan 1965; but see Baker et al. 2003; Foote et al. 1980). We also propose that the strong correlations between LFPs and ERPs represent the strong relationship between aggregate local synaptic processing of target selection in FEF and the neural generator of the m-N2pc, suggesting that LFPs do not reflect only input to a cortical area.

The findings from this combination of techniques provide a step toward understanding the neural basis of selective visual processing across spatial scales and brain areas. Recording ERP components simultaneously with LFPs and single-neuron activity achieves two goals of cognitive neuroscience. First, recording ERPs from macaques performing the same tasks used in studies of humans allows us to bridge the gap between human and nonhuman primate electrophysiology. Second, this combination of methods yields data with excellent spatial and temporal resolution. This has been the goal of combining ERP and imaging methods, although this marriage of neuroscientific techniques uses source estimation procedures that are themselves suggestive, not definitive, due to a number of factors (e.g., Hillyard and Anllo-Vento 1998; Nunez and Srinivasan 2006). Our study shows how hypotheses about the generation of human ERP components can be tested by recording multiple electrophysiological measures from primates exhibiting homologous ERP components. Understanding the neural substrates of noninvasive electrophysiological measures of human cognition is vital for progress in testing psychological theories, treating disorders, and creating brain–computer interfaces.

ACKNOWLEDGMENTS

We thank M. J. Nelson for help with the LFP analysis.

GRANTS

This work was supported by National Institutes of Health Grants T32-MH-064913, T32-EY-007135, R01-EY-08890, P30-EY-08126, and P30-HD-015052; the McKnight Endowment Fund for Neuroscience; and Robin and Richard Patton through the E. Bronson Ingram Chair in Neuroscience.

REFERENCES

Adrian ED, Matthews BHC. The interpretation of potential waves in the cortex. *J Physiol* 81: 440–471, 1934.

Armstrong KM, Fitzgerald JK, Moore T. Changes in visual receptive fields with microstimulation of frontal cortex. *Neuron* 50: 791–798, 2006.

Arthur DL, Starr A. Task-relevant late positive component of the auditory event-related potential in monkeys resembles P300 in humans. *Science* 223: 186–188, 1984.

Baker SN, Curio G, Lemon RN. EEG oscillations at 600 Hz are macroscopic markers for cortical spike bursts. *J Physiol* 550: 529–534, 2003.

Barone P, Batardiere A, Knoblauch K, Kennedy H. Laminar distribution of neurons in extrastriate areas projecting to visual areas V1 and V4 correlates with hierarchical rank and indicates the operation of a distance rule. *J Neurosci* 20: 3263–3281, 2000.

Berger H. Über das elektrenkephalogramm des menschen. *Arch Psychiat Nervenkr* 87: 527–570, 1929.

Bichot NP, Thompson KG, Rao SC, Schall JD. Reliability of macaque frontal eye field neurons signaling saccade targets during visual search. *J Neurosci* 21: 713–725, 2001.

Braitenberg V, Schüz A. *Anatomy of the Cortex: Statistics and Geometry.* Berlin: Springer-Verlag, 1991.

Britten KH, Shadlen MN, Newsome WT, Movshon JA. The analysis of visual motion: a comparison of neuronal and psychophysical performance. *J Neurosci* 12: 4745–4765, 1992.

Bruce CJ, Goldberg ME. Primate frontal eye fields. I. Single neurons discharging before saccades. *J Neurophysiol* 53: 603–635, 1985.

Brunia CHM, Vingerhoets A. CNV and EMG preceding a plantar flexion of the foot. *Biol Psychol* 11: 181–191, 1980.

Buchwald JS, Hala ES, Schramm S. Comparison of multiple-unit and electroencephalogram activity recorded from the same brain sites during behavioural conditioning. *Nature* 205: 1012–1014, 1965.

Bundesen C, Habekost T, Kyllingsbæk S. A neural theory of visual attention: bridging cognition and neurophysiology. *Psychol Rev* 112: 291–328, 2005.

Clark VP, Fan S, Hillyard SA. Identification of early visual evoked potential generators by retinotopic and topographic analyses. *Hum Brain Mapp* 2: 170–187, 1995.

Cohen JY, Heitz RP, Woodman GF, Schall JD. Neural basis of the set-size effect in frontal eye field: timing of attention during visual search. *J Neurophysiol* 101: 1699–1704, 2009a.

Cohen JY, Pouget P, Heitz RP, Woodman GF, Schall JD. Biophysical support for functionally distinct cell types in the frontal eye field. *J Neurophysiol* 101: 912–916, 2009b.

Cohen Y, Cohen JY. *Statistics and Data with R: An Applied Approach Through Examples.* London: Wiley, 2008.

Cooper R, Winter AL, Crow HJ, Walter WG. Comparison of subcortical, cortical and scalp activity using chronically indwelling electrodes in man. *Electroencephalogr Clin Neurophysiol* 18: 217–228, 1965.

Desimone R, Duncan J. Neural mechanisms of selective visual attention. *Annu Rev Neurosci* 18: 193–222, 1995.

Duncan J, Humphreys GW. Visual search and stimulus similarity. *Psychol Rev* 96: 433–458, 1989.

Ebersole JS. Defining epileptic foci: past, present, future. *J Clin Neurophysiol* 14: 470–483, 1997.

Foote SL, Aston-Jones G, Bloom FE. Impulse activity of locus coeruleus neurons in awake rats and monkeys is a function of sensory stimulation and arousal. *Proc Natl Acad Sci USA* 77: 3033–3037, 1980.

Fromm GH, Bond HW. Slow changes in the electrocorticogram and the activity of cortical neurons. *Electroencephalogr Clin Neurophysiol* 17: 520–523, 1964.

Fromm GH, Bond HW. The relationship between neuron activity and cortical steady potentials. *Electroencephalogr Clin Neurophysiol* 22: 159–166, 1967.

Gattass R, Sousa APB, Gross CG. Visuotopic organization and extent of V3 and V4 of the macaque. *J Neurosci* 8: 1831–1845, 1988.

Glover A, Ghilardi MF, Bodis-Wollner IMO, Mylin LH. Visual "cognitive" evoked potentials in the behaving monkey. *Electroencephalogr Clin Neurophysiol* 90: 65–72, 1991.

Gregoriou GG, Gotts SJ, Zhou H, Desimone R. High-frequency, long-range coupling between prefrontal and visual cortex during attention. *Science* 324: 1207–1210, 2009.

Heinze HJ, Mangun GR, Burchert W, Hinrichs H, Scholz M, Münte TF, Gös A, Scherg M, Johannes S, Hundeshagen H, Gazzaniga MS, Hillyard SA. Combined spatial and temporal imaging of brain activity during visual selective attention in humans. *Nature* 372: 543–546, 1994.

Helmholtz H. Ueber einige Gesetze der Vertheilung elektrischer Ströme in körperlichen Leitern mit Anwendung auf die thierisch-elektrischen Versuche. *Ann Physik Chem* 89: 211–233, 354–377, 1853.

Hikosaka O, Wurtz RH. Visual and oculomotor functions of monkey substantia nigra pars reticulata. III. Memory-contingent visual and saccade responses. *J Neurophysiol* 49: 1268–1284, 1983.

Hillyard SA, Anllo-Vento L. Event-related brain potentials in the study of visual selective attention. *Proc Natl Acad Sci USA* 95: 781–787, 1998.

Hillyard SA, Picton TW. Electrophysiology of cognition. In: *Handbook of Physiology. The Nervous System. Higher Functions of the Brain*. Bethesda, MD: Am. J. Physiol., 1987, sect. 1, vol. V, pt. 2, p. 519–584.

Hopf J-M, Boelmans K, Schoenfeld MA, Luck SJ, Heinze H-J. Attention to features precedes attention to locations in visual search: evidence from electromagnetic brain responses in humans. *J Neurosci* 24: 1822–1832, 2004.

Hopf J-M, Luck SJ, Girelli M, Hagner T, Mangun GR, Scheich H, Heinze H-J. Neural sources of focused attention in visual search. *Cereb Cortex* 10: 1233–1241, 2000.

Javitt DC, Schroeder CE, Steinshneider M, Arezzo JC, Vaughan HG. Demonstration of mismatch negativity in the monkey. *Electroencephalogr Clin Neurophysiol* 83: 87–90, 1992.

Juan C-H, Muggleton NG, Tzeng OJL, Hung DL, Cowey A, Walsh V. Segregation of visual selection and saccades in human frontal eye fields. *Cereb Cortex* 18: 2410–2415, 2008.

Katzner S, Nauhaus I, Benucci A, Bonin V, Ringach DL, Carandini M. Local origin of field potentials in visual cortex. *Neuron* 61: 35–41, 2009.

Lachaux JP, Rudrauf D, Kahane P. Intracranial EEG and human brain mapping. *J Physiol* (*Paris*) 97: 613–628, 2003.

Lamme VA, Van Dijk BW, Spekreijse H. Texture segregation is processed by primary visual cortex in man and monkey. Evidence from VEP experiments. *Vision Res* 32: 797–807, 1992.

Lamme VAF, Roelfsema PR. The distinct modes of vision offered by feedforward and recurrent processing. *Trends Neurosci* 23: 571–579, 2000.

Leuthold H, Jentzsch I. Distinguishing neural sources of movement preparation and execution. An electrophysiological analysis. *Biol Psychol* 60: 173–198, 2002.

Logothetis NK, Wandell BA. Interpreting the BOLD signal. *Annu Rev Physiol* 66: 735–769, 2004.

Luck SJ. *An Introduction to the Event-Related Potential Technique.* Cambridge, MA: MIT Press, 2006.

Luck SJ, Girelli M, McDermott MT, Ford MA. Bridging the gap between monkey neurophysiology and human perception: an ambiguity resolution theory of visual selective attention. *Cognit Psychol* 33: 64–87, 1997.

Luck SJ, Hillyard SA. Electrophysiological correlates of feature analysis during visual search. *Psychophysiology* 31: 291–308, 1994a.

Luck SJ, Hillyard SA. Spatial filtering during visual search: evidence from human electrophysiology. *J Exp Psychol Hum Percept Perform* 20: 1000–1014, 1994b.

Marsan CA. Electrical activity of the brain: slow waves and neuronal activity. *Isr J Med Sci* 1: 104–117, 1965.

Mehta AD, Ulbert I, Schroeder CE. Intermodal selective attention in monkeys. I: Distribution and timing of effects across visual areas. *Cereb Cortex* 10: 343–358, 2000a.

Mehta AD, Ulbert I, Schroeder CE. Intermodal selective attention in monkeys. II: Physiological mechanisms of modulation. *Cereb Cortex* 10: 359–370, 2000b.

Michel CM, Murray MM, Lantz G, Gonzalez S, Spinelli L, Grave de Peralta R. EEG source imaging. *Clin Neurophysiol* 115: 2195–2222, 2004.

Monosov IE, Trageser JC, Thompson KG. Measurements of simultaneously recorded spiking activity and local field potentials suggest that spatial selection emerges in the frontal eye field. *Neuron* 57: 614–625, 2008.

Nelson MJ, Pouget P, Nilsen EA, Patten CD, Schall JD. Review of signal distortion through metal microelectrode recording circuits and filters. *J Neurosci Methods* 169: 141–157, 2008.

Nunez PL, Srinivasan R. *Electric Fields of the Brain.* New York: Oxford Univ. Press, 2006.

Orban GA, Van Essen D, Vanduffel W. Comparative mapping of higher visual areas in monkeys and humans. *Trends Cogn Sci* 8: 315–323, 2004.

Paller KA, McCarthy G, Roessler E, Allison T, Wood CC. Potentials evoked in human and monkey medial temporal lobe during auditory and visual oddball paradigms. *Electroencephalogr Clin Neurophysiol* 84: 269–279, 1992.

Pouget P, Stepniewska I, Crowder EA, Leslie MW, Emeric EE, Nelson MJ, Schall JD. Visual and motor connectivity and the distribution of calcium-binding proteins in macaque frontal eye field: implications for saccade target selection. *Front Neuroanat* 3: 2, 2009.

Rockel AJ, Hiorns RW, Powell TPS. The basic uniformity in structure of the neocortex. *Brain* 103: 221–244, 1980.

Rugg MD, Coles MGH. *Electrophysiology of Mind: Event-Related Brain Potentials and Cognition.* Oxford, UK: Oxford Univ. Press, 1995.

Sato T, Murthy A, Thompson KG, Schall JD. Search efficiency but not response interference affects visual selection in frontal eye field. *Neuron* 30: 583–591, 2001.

Sato TR, Schall JD. Effects of stimulus-response compatibility on neural selection in frontal eye field. *Neuron* 38: 637–648, 2003.

Schall JD. On the role of frontal eye field in guiding attention and saccades. *Vision Res* 44: 1453–1467, 2004.

Schall JD, Hanes DP. Neural basis of saccade target selection in frontal eye field during visual search. *Nature* 366: 467–469, 1993.

Schmolesky MT, Wang Y, Hanes DP, Thompson KG, Leutgeb S, Schall JD, Leventhal AG. Signal timing across the macaque visual system. *J Neurophysiol* 79: 3272–3278, 1998.

Schroeder CE, Tenke CE, Givre SJ. Subcortical contributions to the surface-recorded flash-VEP in the awake macaque. *Electroencephalogr Clin Neurophysiol* 84: 219–231, 1992.

Schroeder CE, Tenke CE, Givre SJ, Arezzo JC, Vaughan HGJ. Striate cortical contribution to the surface-recorded pattern-reversal VEP in the alert monkey. *Vision Res* 31: 1143–1157, 1991.

Sereno MI, Dale AM, Reppas JB, Kwong KK, Belliveau JW, Brady TJ, Rosen BR, Tootell RB. Borders of multiple visual areas in humans revealed by functional magnetic resonance imaging. *Science* 268: 889–893, 1995.

Taylor PCJ, Nobre AC, Rushworth MFS. FEF TMS affects visual cortical activity. *Cereb Cortex* 17: 391–399, 2007.

Thompson KG, Bichot NP. A visual salience map in the primate frontal eye field. *Prog Brain Res* 147: 251–262, 2005.

Thompson KG, Bichot NP, Schall JD. Dissociation of visual discrimination from saccade programming in macaque frontal eye field. *J Neurophysiol* 77: 1046–1050, 1997.

Thompson KG, Biscoe KL, Sato TR. Neuronal basis of covert spatial attention in the frontal eye field. *J Neurosci* 25: 9479–9487, 2005.

Thompson KG, Hanes DP, Bichot NP, Schall JD. Perceptual and motor processing stages identified in the activity of macaque frontal eye field neurons during visual search. *J Neurophysiol* 76: 4040–4055, 1996.

Tootell RBH, Hadjikhani N. Where is "dorsal V4" in human visual cortex? Retinotopic, topographic and functional evidence. *Cereb Cortex* 11: 298–311, 2001.

Treisman AM, Gelade G. A feature-integration theory of attention. *Cognit Psychol* 12: 97–136, 1980.

Walter WG. Critical review: the technique and application of electro-encephalography. *J Neurol Psychiatry* 1: 359–385, 1938.

Wolfe JM. Guided search 4.0: current progress with a model of visual search. In: *Integrated Models of Cognitive Systems*, edited by Gray W. New York: Oxford Univ. Press, 2007, p. 99–119.

Woodman GF, Kang M-S, Rossi AF, Schall JD. Nonhuman primate event-related potentials indexing covert shifts of attention. *Proc Natl Acad Sci USA* 104: 15111–15116, 2007.

Woodman GF, Luck SJ. Electrophysiological measurement of rapid shifts of attention during visual search. *Nature* 400: 867–869, 1999.

Woodman GF, Luck SJ. Dissociations among attention, perception, and awareness during object-substitution masking. *Psychol Sci* 14: 605–611, 2003a.

Woodman GF, Luck SJ. Serial deployment of attention during visual search. *J Exp Psychol Hum Percept Perform* 29: 121–138, 2003b.

Zeki SM. Cortical projections from two prestriate areas in the monkey. *Brain Res* 34: 19–35, 1971.